

Phase-controlled coherent dynamics of a single spin under closed-contour interaction

Arne Barfuss, Johannes Kölbl, Lucas Thiel, Jean Teissier, Mark Kasperczyk and Patrick Maletinsky.

In three-level quantum systems, interference between two simultaneously driven excitation pathways can give rise to effects such as coherent population trapping^{1,2} and electromagnetically induced transparency3. The possibility to exploit these effects has made three-level systems a cornerstone of quantum optics. Coherent driving of the third available transition forms a closed-contour interaction (CCI), which yields fundamentally new phenomena, including phase-controlled coherent population trapping4,5 and phase-controlled coherent population dynamics6. Despite attractive prospects, prevalent dephasing in experimental systems suitable for CCI driving has made its observation elusive7-10. Here, we exploit recently developed methods for coherent manipulation of nitrogen-vacancy electronic spins to implement and study highly coherent CCI driving of a single spin. Our experiments reveal phase-controlled quantum interference, reminiscent of electron dynamics on a closed loop threaded by a magnetic flux, which we synthesize from the driving-field phase¹¹. Owing to the nature of the dressed states created under CCI, we achieve nearly two orders of magnitude improvement of the dephasing times, even for moderate drive strengths. CCI driving constitutes a novel approach to coherent control of few-level systems, with potential for applications in quantum sensing or quantum information processing.

Three-level systems, where two of the three available transitions are simultaneously and coherently driven, are used in applications ranging from light storage¹² and atomic clock frequency standards¹³ to coherent quantum control¹⁴⁻¹⁶. Further functionalities could be enabled by closing the interaction contour with a third driving field (Fig. 1a). This would lead to interfering excitation pathways in the system, which depend on the phase of the driving fields and may allow for phase control of electromagnetic susceptibilities or coherent population dynamics⁶. Despite practical interest^{4-6,16}, studying such phase dependence is severely complicated by selection rules that prevent CCI in most experimental systems. Indeed, for symmetry reasons, only two of three available transitions in a threelevel system can be dipole-allowed for the same type of driving field. Earlier experiments exploited a combination of electric and magnetic dipole transitions to overcome this fundamental limitation and study phase-dependent coherent population trapping⁷⁻¹⁰. However, in all of these systems, dephasing rates by far exceeded the rate of coherent manipulation, thereby preventing experimental observation of quantum coherent CCI dynamics thus far.

Here, we overcome these limitations by exploiting recently developed ways to coherently drive the nitrogen-vacancy spin and implement CCI. We establish a strong influence of the driving-field phase on coherent spin dynamics and observe the non-reciprocal

character of CCI in a single three-level system. Due to the unique nature of the emerging dressed states, our CCI scheme allows for a close to two order of magnitude enhancement of the NV's inhomogeneous dephasing time.

The negatively charged NV centre, a substitutional nitrogen atom next to a vacancy in the diamond lattice, forms an S=1 spin system (Fig. 1a) in its orbital ground state. Conveniently, the NV spin can be initialized using optical spin pumping under green laser excitation and optically read out by virtue of its spin-dependent fluorescence¹⁷. The NV's spin sublevels are $|0\rangle$ and $|\pm 1\rangle$, where $|m_s\rangle$ are the eigenstates of the spin operator \hat{S}_z along the NV's symmetry axis z (that is, $\hat{S}_z | m_s \rangle = m_s | m_s \rangle$). In the absence of symmetrybreaking fields, the electronic spin states $|\pm 1\rangle$ are degenerate and shifted from $|0\rangle$ by a zero-field splitting $D_0 = 2.87 \,\text{GHz}$. Applying a static magnetic field B_{NV} along z splits $|\pm 1\rangle$ by $\Delta_z = 2\gamma_{\text{NV}}B_{\text{NV}}$, with $\gamma_{\rm NV} = 2.8 \, \rm MHz \, G^{-1}$, and leads to the formation of the three-level ∇ -system' that we study in this work (Fig. 1a)¹⁸. Although each of the states $|m_s\rangle$ has additional nuclear degrees of freedom due to hyperfine coupling to the NV's ¹⁴N nuclear spin, we restrict ourselves to the hyperfine subspace with nuclear spin quantum number $m_I = +1$ (ref. 19), while other states remain out of resonance with our driving fields and do not contribute to CCI dynamics.

To implement and study CCI dynamics, we employ coherent driving of the NV spin using a combination of time-varying magnetic and strain fields (see Fig. 1). Specifically, we use the well-established method of coherent driving of the $|0\rangle\leftrightarrow|\pm1\rangle$ transitions with microwave magnetic fields²⁰. In addition, we utilize a time-varying strain field to drive the $|-1\rangle\leftrightarrow|+1\rangle$ transition—a recently developed method for efficient, coherent driving of this magnetic dipole-forbidden transition, which is difficult to address otherwise^{19,21}. Considering the combined action of these three driving fields of amplitudes (Rabi frequencies) Ω_i and frequencies ω_i (Fig. 1a), the dynamics of the NV spin in an appropriate rotating frame (see Supplementary Information) are described by the Hamiltonian

$$\widehat{H}_0 = \frac{\hbar}{2} \begin{pmatrix} 2\delta_1 & \Omega_1 & \Omega_3 e^{i\phi} \\ \Omega_1 & 0 & \Omega_2 \\ \Omega_3 e^{-i\phi} & \Omega_2 & 2\delta_2 \end{pmatrix}$$
 (1)

if the three-photon resonance $\omega_1+\omega_3=\omega_2$ is fulfilled (\hbar is the reduced Planck constant). Hamiltonian \widehat{H}_0 is expressed in the basis $\{-1\rangle, |0\rangle, |+1\rangle\}$ and $\delta_{1(2)}$ represent the detunings of the microwave driving fields from the $|0\rangle\leftrightarrow|-1\rangle$ ($|0\rangle\leftrightarrow|+1\rangle$) spin transition. Importantly, and in stark contrast to the usual case of coherent driving of multi-level systems, the resulting spin dynamics are strongly dependent on the phases ϕ_i ($i\in\{1,\ 2,\ 3\}$) of the driving fields,

LETTERS NATURE PHYSICS

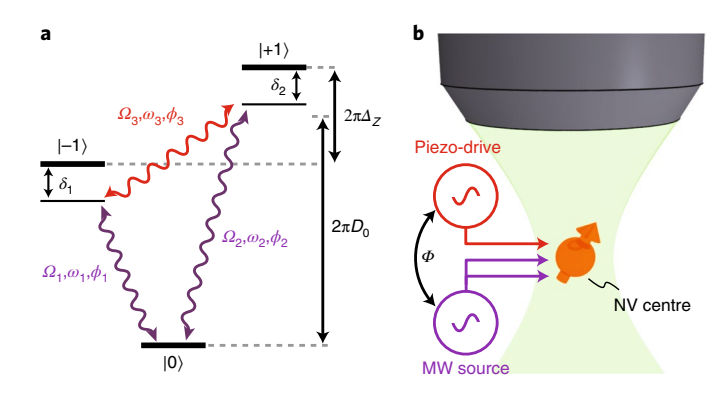


Fig. 1 | The CCI scheme and experimental set-up. **a**, A schematic representation of the three-level CCI system studied here. Levels $|-1\rangle$, $|0\rangle$ and $|+1\rangle$ are the S=1 ground-state spin levels of a negatively charged diamond nitrogen-vacancy (NV) centre. All three possible spin transitions are coherently driven, either by microwave magnetic fields (for $|\Delta m_s| = 1$; purple arrows) or by strain ($|\Delta m_s| = 2$; red arrow). The fields have frequency $ω_p$ amplitude (Rabi frequency) $Ω_p$ and phase $φ_i$ ($i ∈ \{1, 2, 3\}$). **b**, Spin dynamics under CCI are investigated using a confocal microscope for optical initialization and readout of the NV spin. Driving fields for microwave (MW)- and strain-driving are applied through a microwave antenna and piezo-excitation using appropriate generators (see Supplementary Information), which are mutually phase-locked to control the global interaction phase $Φ = φ_1 + φ_3 - φ_2$.

through the gauge-invariant, global phase $\Phi = \phi_1 + \phi_3 - \phi_2$. In the following, we will examine the case of resonant, symmetric driving, for which $\delta_1 = \delta_2 = 0$ and $\Omega_i = \Omega_i \forall i$. In this case, \widehat{H}_0 can be readily diagonalized with resulting dressed eigenstates and eigenenergies

$$|\Psi_k\rangle = \frac{1}{\sqrt{3}} (e^{i(\Phi/3 + 2k\varphi_0)}, 1, e^{-i(\Phi/3 - k\varphi_0)})$$
 (2)

$$E_k/\hbar = \Omega\cos(\Phi/3 - k\varphi_0) \tag{3}$$

with $k \in \{-1, 0, 1\}$ and $\varphi_0 = 2\pi/3$.

To experimentally observe CCI dynamics and generate the required, time-varying strain field, we place a single NV centre in a mechanical resonator of eigenfrequency $\omega_3/2\pi=9.2075$ MHz, which we resonantly drive using a nearby piezo-electric transducer¹⁹. The mechanical Rabi frequency Ω_3 is controlled by the amplitude of the piezo-excitation. To achieve resonant strain driving (that is, $\omega_3/2\pi=\Delta_z$), we apply a static magnetic field $B_{\rm NV}$ along the NV axis. The two microwave magnetic fields used to address the $|0\rangle\leftrightarrow|\pm1\rangle$ transitions at frequencies $\omega_{1,2}=2\pi D_0\pm\omega_3/2$ are delivered to the NV centre using a home-built near-field microwave antenna (see Supplementary Information for more details about phase control and microwave field generation). Finally, a confocal microscope is used for optical initialization and readout of the NV spin (Fig. 1b).

We study the NV spin dynamics under closed-contour driving by measuring the time evolution of the NV spin population for different values of Φ , using the experimental sequence shown in Fig. 2a (inset). For each value of Φ , a green laser pulse initializes the NV spin in $|\psi(\tau=0)\rangle:=|0\rangle=(|\Psi_{-1}\rangle+|\Psi_0\rangle+|\Psi_1\rangle)/\sqrt{3}$, after which we let the system evolve under the influence of the three driving fields for a variable evolution time τ . Finally, we apply a green laser pulse to read out the final population in $|0\rangle$, $P_{|0\rangle}$ (τ)= $|\langle 0|\psi(\tau)\rangle|^2$, where $|\psi(\tau)\rangle=\mathrm{e}^{-i\hat{H}_0\tau/\hbar}$ $|\psi(0)\rangle$. The resulting data (Fig. 2a), here for $\Omega/2\pi=500\,\mathrm{kHz}$, show oscillations of $P_{|0\rangle}$ in time, with a marked π -periodic dependence of the population dynamics on Φ .

To obtain a complete picture of the resulting spin dynamics, we additionally monitor the populations $P_{|\pm|}$ of spin states $|\pm 1\rangle$ for $\Phi=0$ and $\pm\pi/2$ (Fig. 2b) by applying a microwave π -pulse resonant with the $|0\rangle \rightarrow |+1\rangle$ or $|0\rangle \rightarrow |-1\rangle$ transition at the end of the evolution time τ (Ω_{probe} , dashed box in the inset of Fig. 2a). The resulting spin dynamics show that, at $\Phi=\pm\pi/2$, the spin exhibits time-reversal symmetry breaking circulation (Fig. 2b, right) of population between the three states $|0\rangle$, $|+1\rangle$ and $|-1\rangle$ (ref. 11), with a

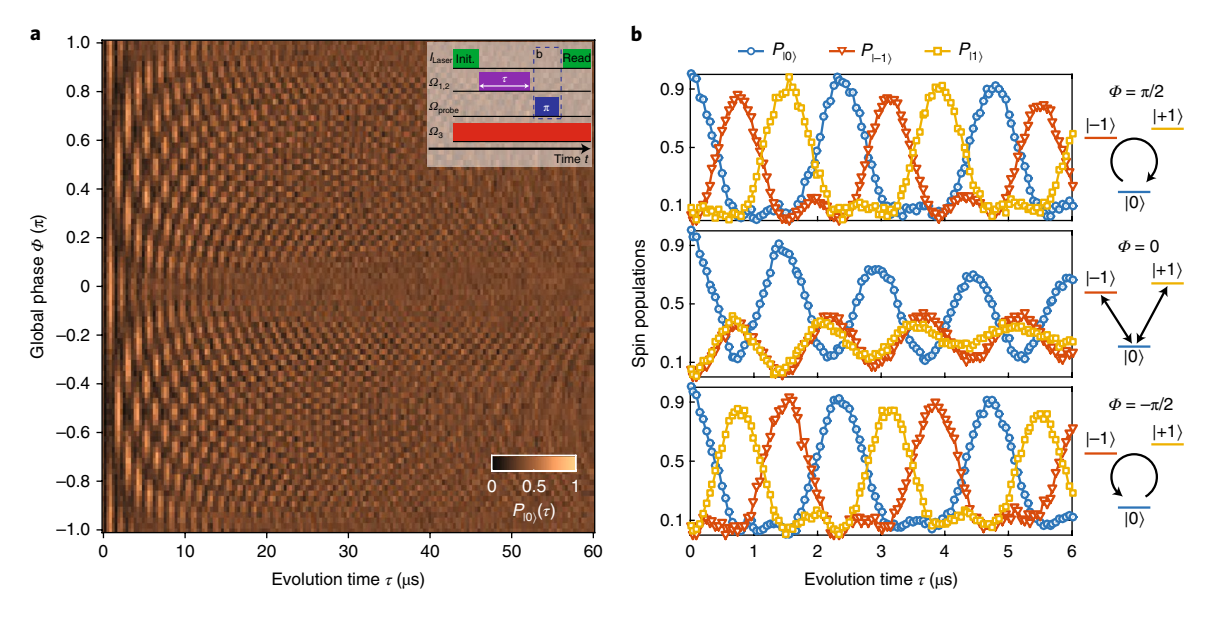


Fig. 2 | Time-reversal symmetry breaking in closed-contour spin dynamics controlled by global phase Φ . **a**, Time evolution of |0⟩ population, $P_{|0⟩}$, as a function of global phase Φ , after initialization in |0⟩. The periodic evolution of $P_{|0⟩}$ is caused by quantum interference in the NV ground state and shows a strong Φ dependence of period and decay times. The inset shows the pulse sequence used for initializing, manipulating and reading out the populations in our system. The dashed box labeled b in the inset indicates that an additional π -pulse is needed to read out the populations of the |-1⟩ and |+1⟩ bare NV states shown in **b**. Readout of the |0⟩ state is accomplished by omitting the π -pulse. **b**, Linecuts of $P_{|m_s⟩}(\tau)$ (with $m_s \in \{-1, 0, +1\}$) for $\Phi = \pi/2$, 0 and $-\pi/2$ (top, middle and bottom panel, respectively). At phases $\Phi = \pm \pi/2$, population shows clockwise or anticlockwise coherent evolutions between the spin sublevels, indicating the non-reciprocal character of the CCI driving. For $\Phi = 0$, the population oscillates between |0⟩ and an equal superposition of $|\pm 1⟩$ (with some admixture of |0⟩).

NATURE PHYSICS LETTERS

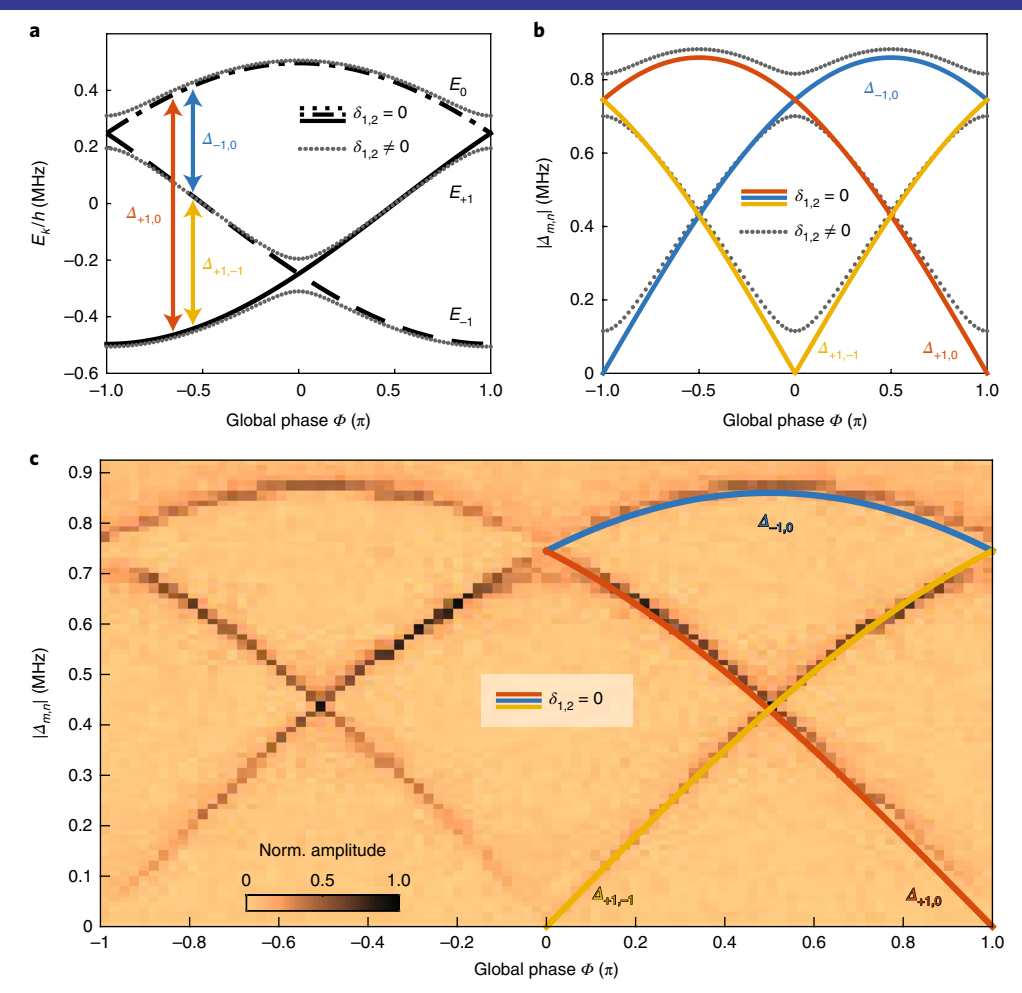


Fig. 3 | Spectrum of the driven NV spin under closed-contour driving. a, Calculated eigenenergies E_k of the driven spin for $\Omega/2\pi$ =500 MHz, as a function of Φ for detuning $\delta_{1,2}$ =0 (black lines) and $\delta_{1,2}/2\pi$ =±50 kHz (dotted lines). **b**, Transition frequencies $|\Delta_{m,n}|$ as a function of Φ for $\delta_{1,2}$ =0 (blue, orange and red lines) and $\delta_{1,2}/2\pi$ =±50 kHz (dotted lines). **c**, Discrete Fourier transform of the data shown in Fig. 2a, as a function of Φ . The spectral components observed agree well with the calculated values of $|\Delta_{m,n}|$; discrepancies around Φ =0,±π arise from environmental magnetic field fluctuations (see text). The observed Fourier amplitude (contrast) is inversely proportional to linewidth and therefore gives an indication of the decay time for each spectral component.

period $T_{\pm\pi/2}=4\pi/\sqrt{3}\,\Omega$. This clockwise and anticlockwise circulation of population, along with its description by Hamiltonian (1), is in perfect analogy with chiral currents of electrons hopping on a plaquette with three sites, threaded by a synthetic magnetic flux Φ . Our observations therefore demonstrate non-reciprocal coherent dynamics controlled by a synthetic gauge field if, created within our CCI driving scheme. Conversely, for $\Phi=0$, the spin-level population oscillates between $|0\rangle$ and an equal superposition of $|\pm 1\rangle$ in a 'V-shaped' trajectory (see Fig. 2b, middle) at a period $T_0=4\pi/3\Omega$. This shortening of T_0 compared to $T_{\pm\pi/2}$ is consistent with the different trajectories (Fig. 2b, right) that the spin populations undergo. To further support that Hamiltonian \widehat{H}_0 provides an accurate description of our system, we calculate the population dynamics and find excellent agreement with data (see Supplementary Information for details of the simulation and comparison with experiment).

In addition to the spin dynamics under CCI, our experiment also allows us to directly access the eigenenergies E_k of the driven three-level system (see equation (3) and the black lines in Fig. 3a). After initialization into $|0\rangle = (|\Psi_{-1}\rangle + |\Psi_0\rangle + |\Psi_1\rangle)/\sqrt{3}$, each component $|\Psi_k\rangle$ acquires a dynamical phase $E_k\tau/\hbar$, which governs the time evolution of the NV spin. The population $P_{|0\rangle}(\tau)$ therefore shows spectral components at frequencies $\Delta_{m,n} = (E_m - E_n)/\hbar$ with $m \neq n \in \{-1, 0, 1\}$ (Fig. 3a,b). A Fourier transformation of $P_{|0\rangle}(\tau)$ (Fig. 3c) thus

reveals $\Delta_{m,n}$ and thereby the eigenenergies of the driven NV spin, which for most values of Φ are in excellent agreement with the predictions based on \widehat{H}_0 (coloured lines in Fig. 3c). Around $\Phi = 0$ and $\pm \pi$, we find anti-crossings instead of the expected frequency crossings in the spectrum, an observation we assign to environmental fluctuations and slow drifts. Indeed, the resulting, non-resonant or asymmetric drive lifts the degeneracies of the dressed states and explains our observation (Fig. 3a,b). Taking these effects into account, we conducted numerical modelling of our experiment and found good qualitative agreement with our observed spectra (see Supplementary Information).

The effect of environmental fluctuations is already visible in the phase-dependent interference patterns in Fig. 2a, where the resulting quantum beats decay fastest for phase-values close to $\Phi=0$ and $\pm\pi$ —an indication that, at these phase values, the dressed states $|\Psi_k\rangle$ are most vulnerable to environmental fluctuations, but protected from them at other values of Φ . Figure 4a shows linecuts taken at $\Phi=0$ (top panel) and $\Phi=-\pi/4$ (bottom panel), which evidence a dramatic change of the dressed-state coherence time from $T_{-1,0}^{\rm dec}=(8.5\pm1.9)~\mu{\rm s}$ at $\Phi=0$ to $T_{-1,0}^{\rm dec}=(124.8\pm28.3)~\mu{\rm s}$ at $\Phi=-\pi/4$. To systematically quantify this Φ -dependent dephasing, we fit a sum of three exponentially decaying sinusoids to the time traces in Fig. 2a and extract decay times $T_{m,n}^{\rm dec}$ for each frequency component $\Delta_{m,n}$.

LETTERS NATURE PHYSICS

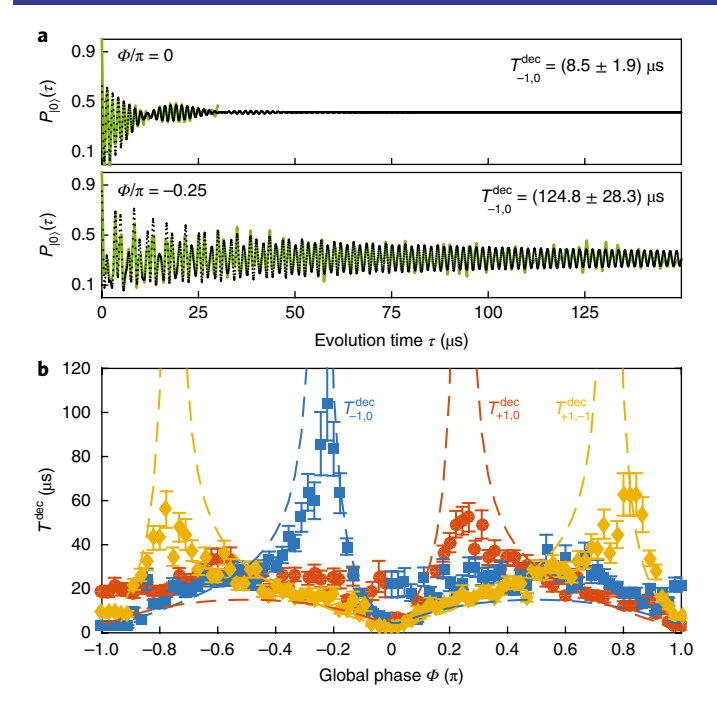


Fig. 4 | Phase-controlled coherence protection. a, Spin oscillations under closed-contour driving for $\Phi=0$ and $\Phi=-\pi/4$, revealing strongly phase-dependent decay times $T_{m,n}^{\rm dec}(\Phi)$. A fit of exponentially damped harmonics (see text) yields $T_{-1,0}^{\rm dec}(\Phi=0)=8.5\pm1.9\,\mu {\rm s}$, and $T_{-1,0}^{\rm dec}(\Phi=-\pi/4)=124.8\pm28.3\,\mu {\rm s}$ for the most long-lived spectral components. **b,** Systematic measurement of decay times as a function of Φ , showing minima of $T_{m,n}^{\rm dec}(\Phi)$ at $\Phi/\pi=\pm1$, 0 and pronounced maxima at $\Phi\approx\pm n\pi/4$, $n\in 1$, 3. The dashed lines are the results of a second-order perturbative calculation of $T_{m,n}^{\rm dec}(\Phi)$ (see text). Note that data in **a** and **b** originate from separate measurement runs and therefore result in slight differences in decay times. All error bars represent 95% confidence intervals for the nonlinear least-squares parameter estimates to our experimental data.

The resulting dependence of $T_{m,n}^{\text{dec}}$ on Φ is shown in Fig. 4b, and exhibits pronounced maxima of Rabi decay times at $\Phi \approx \pm n\pi/4$, $n \in \{1, 3\}$ (see Supplementary Information).

Our data suggest that compared to prior work on coherence protection by continuous driving 19,22-24, dressed states in CCI driving can be efficiently decoupled from environmental magnetic noise at comparatively weak driving fields $\Omega \approx 500$ kHz. Since the three $|\Psi_k\rangle$ are equally weighted superpositions of the three NV spin sublevels, they carry zero total angular momentum and are insensitive to magnetic fields to first order, except near the singular degeneracy points at $\Phi = 0$, $\pm \pi$. To understand the decoupling mechanism and its phase dependence in detail, we conducted extensive numerical modelling together with perturbative, analytical calculations of $T_{m,n}^{\text{dec}}(\Phi)$ (see Supplementary Information). Our second-order perturbative calculations account for magnetic field fluctuations with Ornstein-Uhlenbeck statistics, together with a random field that was held static over each experimental run. The result (dashed lines in Fig. 4b) reveals that, for each of the values $\Phi \approx \pm \pi/4$ and $\pm 3\pi/4$, two dressed states exist whose energies show the same perturbative response to magnetic field fluctuations and thus form a coherence-protected subspace in the dressed state manifold, in which $T_{m,n}^{\text{dec}}(\Phi)$ approaches the spin relaxation time. We assign the significantly reduced, measured value $T_{-1,0}^{\text{dec}}(-\pi/4) \approx 105 \,\mu\text{s}$ to driving field fluctuations—a hypothesis that we could quantitatively support with our numerical modelling (see Supplementary Information). Our data also show that the four local maxima of $T_{m,n}^{\text{dec}}$ vary significantly in magnitude. We attribute this variation to slow

experimental drifts of the zero-field splitting parameter D_0 due to temperature variations²⁵ in our experiment. Taking these drifts into account in our model yields excellent agreement between simulation and experiment for realistic temperature variations of ± 1.3 K (see Supplementary Information).

Our results establish the driving-field phase under CCI driving as a novel control parameter for coherent manipulation and dynamical decoupling of single spins. They indicate that further experimental improvements would readily yield coherence protected dressed states with inhomogeneous dephasing times approaching the T_1 limit. Such dressed states have recently been established as powerful resources for quantum sensing of gigahertz fields^{26,27}. The efficient tunability and coherence protection we demonstrate for dressed states offer interesting avenues for enhanced sensitivities and phase-tuning of the sensing frequencies in such sensing schemes. In addition, applications of CCI in quantum information processing could be explored in conjunction with initialization and coherent manipulation of dressed states, or their coherent coupling to nearby nuclear spins²⁸. Lastly, we note the strong analogy between the non-reciprocal spin dynamics under CCI driving we demonstrated and recent realizations of synthetic gauge fields in optomechanical systems²⁹. Pursuing this analogy using ensembles of NV centres with engineered dissipation offers interesting avenues for realizing on-chip, non-reciprocal microwave elements, such as microwave circulators or directional amplifiers29.

Data availability. The data sets generated and/or analysed during this study are available from the corresponding author on request.

Received: 6 February 2018; Accepted: 22 June 2018; Published online: 6 August 2018

References

- Gray, H. R., Whitley, R. M. & Stroud, C. R. Coherent trapping of atomic populations. Opt. Lett. 3, 218–220 (1978).
- Agapèv, B. D., Gorny, M. B., Matisov, B. G. & Rozhdestvenski, Y. V. Coherent population trapping in quantum systems. *Phys.-Uspekhi* 36, 763–793 (1993).
- Fleischhauer, M., Imamoglu, A. & Marangos, J. P. Electromagnetically induced transparency: Optics in coherent media. Rev. Mod. Phys. 77, 633–673 (2005).
- Kosachiov, D. V., Matisov, B. G. & Rozhdestvensky, Y. V. Coherent phenomena in multilevel systems with closed interaction contour. *J. Phys. B* 25, 2473–2488 (1992).
- Windholz, L. Coherent population trapping in multi-level atomic systems. Phys. Scr. 2001, 81–91 (2001).
- Buckle, S., Barnett, S., Knight, P., Lauder, M. & Pegg, D. Atomic interferometers. Opt. Acta 33, 1129–1140 (1986).
- Yamamoto, K., Ichimura, K. & Gemma, N. Enhanced and reduced absorptions via quantum interference: Solid system driven by a rf field. *Phys. Rev. A* 58, 2460–2466 (1998).
- Korsunsky, E. A., Leinfellner, N., Huss, A., Baluschev, S. & Windholz, L. Phase-dependent electromagnetically induced transparency. *Phys. Rev. A* 59, 2302–2305 (1999).
- Li, H. et al. Electromagnetically induced transparency controlled by a microwave field. Phys. Rev. A 80, 023820 (2009).
- Preethi, T. M. et al. Phase-sensitive microwave optical double resonance in an N system. EPL Europhys. Lett. 95, 34005 (2011).
- 11. Roushan, P. et al. Chiral ground-state currents of interacting photons in a synthetic magnetic field. *Nat. Phys.* **13**, 146–151 (2017).
- Phillips, D. F., Fleischhauer, A., Mair, A., Walsworth, R. L. & Lukin, M. D. Storage of light in atomic vapor. *Phys. Rev. Lett.* 86, 783–786 (2001).
- Vanier, J. Atomic clocks based on coherent population trapping: a review. Appl. Phys. B 81, 421–442 (2005).
- Cirac, J. I., Zoller, P., Kimble, H. J. & Mabuchi, H. Quantum state transfer and entanglement distribution among distant nodes in a quantum network. *Phys. Rev. Lett.* 78, 3221–3224 (1997).
- Northup, T. E. & Blatt, R. Quantum information transfer using photons. Nat. Photon. 8, 356–363 (2014).
- Shore, B. W. Manipulating Quantum Structures Using Laser Pulses (Cambridge Univ. Press, Cambridge, 2011)
- Gruber, A. et al. Scanning confocal optical microscopy and magnetic resonance on single defect centers. Science 276, 2012–2014 (1997).

NATURE PHYSICS LETTERS

- Doherty, M. W. et al. The nitrogen-vacancy colour centre in diamond. *Phys. Rep.* 528, 1–45 (2013).
- Barfuss, A., Teissier, J., Neu, E., Nunnenkamp, A. & Maletinsky, P. Strong mechanical driving of a single electron spin. Nat. Phys. 11, 820–824 (2015).
- Dobrovitski, V., Fuchs, G., Falk, A., Santori, C. & Awschalom, D. Quantum control over single spins in diamond. *Annu. Rev. Condens. Matter Phys.* 4, 23–50 (2013).
- 21. MacQuarrie, E. R. et al. Coherent control of a nitrogen–vacancy center spin ensemble with a diamond mechanical resonator. *Optica* **2**, 233–238 (2015).
- Cai, J.-M. et al. Robust dynamical decoupling with concatenated continuous driving. New J. Phys. 14, 113023 (2012).
- 23. Xu, X. et al. Coherence-protected quantum gate by continuous dynamical decoupling in diamond. *Phys. Rev. Lett.* **109**, 070502 (2012).
- MacQuarrie, E. R., Gosavi, T. A., Bhave, S. A. & Fuchs, G. D. Continuous dynamical decoupling of a single diamond nitrogen-vacancy center spin with a mechanical resonator. *Phys. Rev. B* 92, 224419 (2015).
- Acosta, V. M. et al. Temperature dependence of the nitrogen-vacancy magnetic resonance in diamond. *Phys. Rev. Lett.* 104, 070801 (2010).
- Joas, T., Waeber, A. M., Braunbeck, G. & Reinhard, F. Quantum sensing of weak radio-frequency signals by pulsed Mollow absorption spectroscopy. *Nat. Commun.* 8, 964 (2017).
- Stark, A. et al. Narrow-bandwidth sensing of high-frequency fields with continuous dynamical decoupling. Nat. Commun. 8, 1105 (2017).
- 28. Abobeih, M. H., One-second coherence for a single electron spin coupled to a multi-qubit nuclear-spin environment. *Nat. Commun.* **9**, 2552 (2018).
- Fang, K. et al. Generalized non-reciprocity in an optomechanical circuit via synthetic magnetism and reservoir engineering. Nat. Phys. 13, 465–471 (2017).

Acknowledgements

We thank A. Retzker, N. Aharon, A. Nunnenkamp and H. Ribeiro for fruitful discussions and valuable input. We gratefully acknowledge financial support through the NCCR QSIT, a competence centre funded by the Swiss NSF, through the Swiss Nanoscience Institute, by the EU FP7 project DIADEMS (grant no. 611143) and through SNF Project Grant 169321.

Author contributions

A.B., J.T. and P.M conceived the experiment. A.B. and J.K. performed the experiment and analysed the data, together with M.K. and P.M.. L.T. and J.T. provided support in measurement software. A.B. and M.K. performed the theoretical modelling of our data. A.B., M.K. and P.M. wrote the paper.

Competing interests

The authors declare no competing interests.

Additional information

Supplementary information is available for this paper at https://doi.org/10.1038/s41567-018-0231-8.

Reprints and permissions information is available at www.nature.com/reprints.

Correspondence and requests for materials should be addressed to P.M.

Publisher's note: Springer Nature remains neutral with regard to jurisdictional claims in published maps and institutional affiliations.